A peer-reviewed version of this preprint was published in PeerJ on 1 December 2017.

View the peer-reviewed version (peerj.com/articles/4088), which is the preferred citable publication unless you specifically need to cite this preprint.

Gehan MA, Fahlgren N, Abbasi A, Berry JC, Callen ST, Chavez L, Doust AN, Feldman MJ, Gilbert KB, Hodge JG, Hoyer JS, Lin A, Liu S, Lizárraga C, Lorence A, Miller M, Platon E, Tessman M, Sax T. 2017. PlantCV v2: Image analysis software for high-throughput plant phenotyping. PeerJ 5:e4088 https://doi.org/10.7717/peerj.4088

PlantCV v2.0: Image analysis software for high-throughput plant phenotyping

Malia A Gehan[*, 1], Noah Fahlgren[*, 1], Arash Abbasi[1], Jeffrey C Berry[1], Steven T Callen[1, 2], Leonardo Chavez[1], Andrew N Doust[3], Max J Feldman[1], Kerrigan B Gilbert[1], John G Hodge[3], J Steen Hoyer[1, 4], Andy Lin[1, 5], Suxing Liu[6, 7], César Lizárraga[1, 8], Argelia Lorence[9], Michael Miller[1, 10], Eric Platon[11], Monica Tessman[1, 2], Tony Sax[12]

[1] Donald Danforth Plant Science Center, St. Louis, Missouri, United States of America

[2] Current Address: Monsanto Company, St. Louis, Missouri, United States of America

[3] Department of Plant Biology, Ecology, and Evolution, Oklahoma State University, Stillwater, Oklahoma, United States of America

[4] Computational and Systems Biology Program, Washington University in St. Louis, St. Louis, Missouri, United States of America

[5] Current Address: Unidev, St. Louis, Missouri, United States of America

[6] Arkansas Biosciences Institute, Arkansas State University, Jonesboro, Arkansas, United States of America

[7] Current Address: Department of Plant Biology, University of Georgia, Athens, Georgia, United States of America

[8] Current Address: CiBO Technologies, Cambridge, Massachusetts, United States of America

[9] Arkansas Biosciences Institute, Department of Chemistry and Physics, Arkansas State University, Jonesboro, Arkansas, United States of America

[10] Current Address: Department of Agronomy and Horticulture, Center for Plant Science Innovation, Beadle Center for Biotechnology, University of Nebraska - Lincoln, Lincoln, Nebraska, United States of America

[11] Cosmos X, Tokyo, Japan

[12] Missouri University of Science and Technology, Rolla, Missouri, United States of America

* These authors contributed equally to this work

Corresponding Author:

Malia Gehan; Noah Fahlgren

975 North Warson Road, St. Louis, MO 63132, USA

Email address: mgehan@danforthcenter.org; nfahlgren@danforthcenter.org

ABSTRACT

Systems for collecting image data in conjunction with computer vision techniques are a powerful tool for increasing the temporal resolution at which plant phenotypes can be measured non-destructively. Computational tools that are flexible and extendable are needed to address the diversity of plant phenotyping problems. We previously described the Plant Computer Vision (PlantCV) software package, which is an image processing toolkit for plant phenotyping analysis. The goal of the PlantCV project is to develop a set of modular, reusable, and repurposable tools for plant image analysis that are open-source and community-developed. Here we present the details and rationale for major developments in the second major release of PlantCV. In addition to overall improvements in the organization of the PlantCV project, new functionality includes a set of new image processing and normalization tools, support for analyzing images that include multiple plants, leaf segmentation, landmark identification tools for morphometrics, and modules for machine learning.

INTRODUCTION

All approaches for improving crops eventually require measurement of traits (phenotyping) (Fahlgren, Gehan & Baxter, 2015). However, manual plant measurements are time-consuming and often require destruction of plant materials in the process, which prevents measurement of traits for a single plant through time. Consequently, plant phenotyping is widely recognized as a major bottleneck in crop improvement (Furbank & Tester, 2011). Targeted plant phenotypes can range from measurement of gene expression, to flowering time, to grain yield; therefore, the software and hardware tools used are often diverse. Here, we focus on the software tools required to nondestructively measure plant traits through images. This is a challenging area of research because the visual definition of phenotypes vary depending on the target species. For example, for identification of flowering time, floral structures might be yellow like those of *Camelina sativa* but also can be green like those of *Brachypodium distachyon*. Therefore, software tools needed to process high-throughput image data need to be flexible and amenable to community input.

The term 'high-throughput' is relative to the difficulty to collect the measurement. The scale that might be considered high-throughput for root phenotyping might not be the same for shoot phenotyping, which can be technically easier to collect depending on the trait and species. Here we define high-throughput as thousands or hundreds of thousands of images per dataset. PlantCV is an open-source, open-development suite of analysis tools capable of analyzing high-throughput image-based phenotyping data (Fahlgren et al., 2015). Version 1.0 of PlantCV (PlantCV v1.0) was released in 2015 alongside the introduction of the Bellwether Phenotyping Facility at the Donald Danforth Plant Science Center (Fahlgren et al., 2015). PlantCV v1.0 was

envisioned as a base suite of tools that the community could build upon, which lead to several design decisions aimed at encouraging participation. First, GitHub was used as a platform to organize the community by integrating version control, code distribution, documentation, issue tracking, and communication between users and contributors (Perez-Riverol et al., 2016). Second, PlantCV was written in Python, a high-level language widely used for both teaching and bioinformatics (Mangalam, 2002; Dudley & Butte, 2009), to facilitate contribution from both biologists and computer scientists. Additionally, the use of Python allows extension of PlantCV with the many tools available from the Python scientific computing community (Oliphant, 2007; Millman & Aivazis, 2011). Third, a focus on modular development fosters code reuse and makes it easier to integrate PlantCV with new or existing systems. Finally, the use of a permissive, open-source license (MIT) allows PlantCV to be used, reused, or repurposed with limited restrictions, for both academic and proprietary applications. The focus of the paper associated with the original release of PlantCV v1.0 (Fahlgren et al., 2015) was not the structure and function of PlantCV for image analysis, but rather an example of the type of biological question that can be answered with high-throughput phenotyping hardware and software platforms. Since the release of PlantCV v1.0 major changes have been made to increase the flexibility, usability, and functionality of PlantCV. Here we document the structure of PlantCV v2.0 along with examples that demonstrate new functionality.

RESULTS AND DISCUSSION

The following are details on improvements to the structure, usability, and functionality of PlantCV since the v1.0 release. Further documentation for using PlantCV can be found at the project website (http://plantcv.danforthcenter.org/).

92 **Organization of the PlantCV project**

93 PlantCV is made up of modular Python functions, which are reusable units of Python code with
94 defined inputs and outputs (Fig. 1). PlantCV functions can be assembled into simple sequential
95 or branching/merging pipelines. A pipeline can be as long or as short as it needs to be, allowing
96 for maximum flexibility for users using different imaging systems and analyzing features of
97 seed, shoot, root, or other plant systems. Each function has a debugging option to allow users to
98 view and evaluate the output of a single step and adjust parameters as necessary. Once a
99 satisfactory pipeline script is developed, the PlantCV parallelization script can be used to deploy
100 the pipeline across a large set of image data (Fig. 1). The parallelization script also functions to
101 manage data by consolidating measurements and metadata into an SQLite database (Fig. 1). In
102 terms of speed, the user is only limited by the complexity of the pipeline and the number of
103 available processors.
104
105 The modular structure of the PlantCV package makes it easier for members of the community to
106 become contributors. Contributors to PlantCV submit bug reports, develop new functions, or
107 extend existing functionality or documentation. Core PlantCV developers do not filter additions
108 of new functions in terms of perceived impact or number of users but do check that new
109 functions follow the PlantCV contribution guide, which can be found in the PlantCV GitHub
110 repository and in the online documentation (http://plantcv.danforthcenter.org). PlantCV
111 contributors are asked to follow the PEP8 Python style guide
112 (https://www.python.org/dev/peps/pep-0008/). Additions or revisions to the PlantCV code or
113 documentation are submitted for review using pull requests via GitHub. The pull request
114 mechanism is essential to protect against merge conflicts, which are sections of code that have

been edited by multiple users in potentially incompatible ways. In PlantCV v2.0, several service integrations were added to automate common tasks during pull requests and updates to the code repository. A continuous integration framework using the Travis CI service (https://travis-ci.org/) was added so that software builds and unit tests can be run automatically upon pull requests and other software updates. Continuous integration provides a safeguard against code updates that break existing functionality by providing a report that shows which tests passed or failed for each build (Wilson et al., 2014). The effectiveness of continuous integration depends on having thorough unit test coverage of the PlantCV code base. Unit test coverage of the PlantCV Python package is monitored through the Coveralls service (https://coveralls.io/), which provides a report on which parts of the code are covered by existing unit tests. In addition to the code, the PlantCV documentation was updated to use a continuous documentation framework using the Read the Docs service (https://readthedocs.org/), which allows documentation to be updated automatically and versioned in parallel with updates to PlantCV. The documentation was updated to cover all functions in the PlantCV library, tutorials on building pipelines and using specialized tools (e.g. multi-plant analysis and machine learning tools), a frequently asked questions section, and several guides such as installation, Jupyter notebooks, and instructions for contributors.

Improved usability

PlantCV v1.0 required pipeline development to be done using the command line, where debug mode is used to write intermediate image files to disk for each step. In command-line mode, the entire pipeline script must be executed, even if only a single step is being evaluated. To improve the pipeline and function development process in PlantCV v2.0, the debugging system was

updated to allow for seamless integration with the Juptyer Notebook system (http://jupyter.org/) (Kluyver et al., 2016). Jupyter compatibility allows users to immediately visualize output and to iteratively rerun single steps in a multi-step PlantCV pipeline, which makes parameters like thresholds or regions of interest much easier to adjust. Once a pipeline is developed in Jupyter, it is relatively straightforward to convert the notebook into a PlantCV pipeline script (see the online documentation). Jupyter notebooks are also a convenient method of sharing pipelines with collaborators and can be downloaded in multiple formats for publication purposes. Jupyter notebooks are also a helpful tool to teach others to use PlantCV.

PlantCV was initially created to analyze data generated by the Bellwether Phenotyping Facility at the Donald Danforth Plant Science Center. Several updates to PlantCV v2.0 addressed the need to increase the flexibility of PlantCV to analyze data from other plant phenotyping systems. The PlantCV SQLite database schema was simplified so that new tables do not need to be added for every new camera system. The full database schema is available on GitHub (see Materials and Methods). New utilities were added to PlantCV v2.0 that allow data to be quickly and efficiently exported from the SQLite database into text files that are compatible with R (R Core Team, 2017) for further statistical analysis and data visualization.

Because standards for data collection and management for plant phenotyping data are still being developed (Pauli et al., 2016), image metadata is often stored in a variety of formats on different systems. A common approach is to include metadata within image filenames, but because there is a lack of file naming standards, it can be difficult to robustly capture this data automatically. In PlantCV v2.0, a new metadata processing system was added to allow for flexibility in file

naming both within and between experiments and systems. The PlantCV metadata processing system is part of the parallelization tool and works by using a user-provided template to process filenames. User-provided templates are built using a restricted vocabulary so that metadata can be collected in a standardized way. The vocabulary used can be easily updated to accommodate future community standards.

Performance

In PlantCV v1.0, image analysis parallelization was achieved using a Perl-based multi-threading system that was not thread-safe, which occasionally resulted in issues with data output that had to be manually corrected. Additionally, the use of the Python package Matplotlib (Hunter, 2007) in PlantCV v1.0 limited the number of usable processors to 10-12. For PlantCV v2.0, the parallelization framework was completely rewritten in Python using a multiprocessing framework, and the use of Matplotlib was updated to mitigate the issues and processor constraints in v1.0. The output of image files mainly used to assess image segmentation quality is now optional, which should generally increase computing performance. Furthermore, to decentralize the computational resources needed for parallel processing and prepare for future integration with high-throughput computing resources that use file-in-file-out operations, results from PlantCV pipeline scripts (one per image) are now written out to temporary files that are aggregated by the parallelization tool after all image processing is complete.

New Functionality

PlantCV v2.0 has added new functions for image white balancing, auto-thresholding, size marker normalization, multi-plant detection, combined image processing, watershed segmentation,

184 landmarking, and a trainable naive Bayes classifier for image segmentation (machine learning).
185 The following are short descriptions and sample applications of new PlantCV functions.
186
187 *White balancing*
188 If images are captured in a greenhouse, growth chamber, or other situation where light intensity
189 is variable, image segmentation based on global thresholding of image intensity values can
190 become variable. To help mitigate image inconsistencies that might impair the ability to use a
191 single global threshold and thus a single pipeline over a set of images, a white balance function
192 was developed. If a white color standard is visible within the image, the user can specify a region
193 of interest. If a specific area is not selected then the whole image is used. Each channel of the
194 image is scaled relative to the reference maximum.
195
196 *Auto-thresholding functions*
197 An alternative approach to using a fixed, global threshold for image segmentation is to use an
198 auto-thresholding technique that either automatically selects an optimal global threshold value or
199 introduces a variable threshold for different regions in an image. Triangle, Otsu, mean, and
200 Gaussian auto-thresholding functions were added to PlantCV to further improve object detection
201 when image light sources are variable. The 'triangle_auto_threshold' function implements the
202 method developed by Zack et al. 1977 (Zack, Rogers & Latp, 1977). The triangle threshold
203 method uses the histogram of pixel intensities to differentiate the target object (plant) from
204 background by generating a line from the peak pixel intensity (Duarte, 2015) to the last pixel
205 value and then finding the point (i.e., the threshold value) on the histogram that maximizes
206 distance to that line. In addition to producing the thresholded image in debug mode, the

207 'triangle_auto_threshold' function outputs the calculated threshold value and the histogram of
208 pixel intensities that was used to calculate the threshold. In cases where the auto-threshold value
209 does not adequately separate the target object from background, the threshold can be adjusted by
210 modifying the stepwise input. Modifying the stepwise input shifts the distance calculation along
211 the x-axis, which subsequently calculates a new threshold value to use.
212
213 The Otsu, mean, and Gaussian threshold functions in PlantCV are implemented using the
214 OpenCV library (Bradski, 2000). Otsu's binarization ['otsu_auto_threshold;' (Otsu, 1979)] is
215 best implemented when a grayscale image histogram has two peaks since the Otsu method
216 selects a threshold value that minimizes the weighted within-class variance. In other words, the
217 Otsu method identifies the value between two peaks where the variances of both classes are
218 minimized. Mean and Gaussian thresholding are executed by indicating the desired threshold
219 type in the function 'adaptive_threshold.' The mean and Gaussian methods will produce a
220 variable local threshold where the threshold value of a pixel location depends on the intensities
221 of neighboring pixels. For mean adaptive thresholding, the threshold of a pixel location is
222 calculated by the mean of surrounding pixel values; for Gaussian adaptive thresholding, the
223 threshold value of a pixel is the weighted sum of neighborhood values using a Gaussian window
224 (Gonzalez & Woods, 2002; Kaehler & Bradski, 2016).
225
226 *Gaussian blur*
227 In addition to the 'median_blur' function included in PlantCV v1.0, we have added a Gaussian
228 blur smoothing function to reduce image noise and detail. Both the median and Gaussian blur
229 methods are implemented using the OpenCV library (Bradski, 2000) and are typically used to

smooth a binary image that has been previously thresholded. Utilizing a rectangular neighborhood around a center pixel, 'median_blur' replaces each pixel in the neighborhood with the median value. Alternatively, 'gaussian_blur' determines the value of the central pixel by multiplying its and neighboring pixel values by a normalized kernel and then averaging these weighted values (i.e., image convolution) (Kaehler & Bradski, 2016). The extent of image blurring can be modified by increasing (for greater blur) or decreasing the kernel size (which takes only odd numbers; commonly, 3x3) or by changing the standard deviation in the X and/or Y directions.

Size marker normalization

Images that are not collected from a consistent vantage point require one or more size markers as references for absolute or relative scale. The size marker function allows users to either detect a size marker within a user-defined region of interest or to select a specific region of interest to use as the size marker. The pixel area of the marker is returned as a value that can be used to normalize measurements to the same scale. For this module to function correctly we assume that the size marker stays in frame, is unobstructed, and is relatively consistent in position throughout a dataset, though some movement is allowed as long as the marker remains within the defined marker region of interest.

Multi-plant detection

There is growing interest among the PlantCV user community to process images with multiple plants grown in flats or trays, but PlantCV v1.0 was built to processes images containing single plants. The major challenge with analyzing multiple plants in an image is successfully

identifying individual whole plants as distinct objects. Leaves or other plant parts can sometimes be detected as distinct contours from the rest of the plant and need to be grouped with other contours from the same plant to correctly form a single plant/target object. While creating multiple regions of interest (ROI) to demarcate each area containing an individual plant/target is an option, we developed two modules, 'cluster_contours' and 'cluster_contours_split_img,' that allow contours to be clustered and then parsed into multiple images without having to manually create multiple ROIs (Fig. 2).

The 'cluster_contours' function takes as input: an image, the contours that need to be clustered, a number of rows, and a number of columns. Total image size is detected, and the rows and columns create a grid to serve as approximate ROIs to cluster the contours. The number of rows and columns approximate the desired size of the grid cells. There does not need to be an object in each of the grid cells. Several functions were also added to aid the clustering function. The 'rotate_img' and 'shift_img' functions allow the image to be adjusted so objects are better aligned to a grid pattern.

After objects are clustered, the 'cluster_contour_split_img' function splits images into the individual grid cells and outputs each as a new image so that there is a single clustered object per image. If there is no clustered object in a grid cell, no image is outputted. With the 'cluster_contour_split_img' function, a text file with genotype names can be included to add them to image names. The 'cluster_contour_split_img' function also checks that there are the same number of names as objects. If there is a conflict in the number of names and objects, a warning is printed and a correction is attempted. Alternatively, if the file option is not used, all of

the object groups are labeled by position. Once images are split, they can be processed like single plant images using additional PlantCV tools. See the online documentation for an example multi-plant imaging pipeline (http://plantcv.readthedocs.io/en/latest/multi-plant_tutorial/).

The current method for multi-plant identification in PlantCV is flexible but relies on a grid arrangement of plants, which is common for controlled-environment-grown plants. Future releases of PlantCV may incorporate additional strategies for detection and identification of plants, such as arrangement-independent *K*-means clustering approaches (Minervini, Abdelsamea & Tsaftaris, 2014).

Combined image processing

The Bellwether Phenotyping Facility has both RGB visible light (VIS) and near-infrared (NIR) cameras, and images are captured ~1 minute apart (Fahlgren et al., 2015). Compared to VIS images, NIR images are grayscale with much less contrast between object and background. It can be difficult to segment plant material from NIR images directly, even with edge detection steps. Therefore, several functions were added to allow the plant binary mask that results from VIS image processing pipelines to be resized and used as a mask for NIR images. Combining VIS and NIR camera pipelines also has the added benefit of decreasing the number of steps necessary to process images from both camera types, thus increasing image processing throughput. The 'get_nir' function identifies the path of the NIR image that matches VIS image. The 'get_nir' function requires that the image naming scheme is consistent and that the matching image is in the same image directory. The 'resize' function then resizes the VIS plant mask in both the x and y directions to match the size of the NIR image. Resizing values are determined by measuring

the same reference object in an example image taken from both VIS and NIR cameras (for example the width of the pot or pot carrier in each image). The 'crop_position_mask' function is then used to adjust the placement of the VIS mask over the NIR image and to crop/adjust the VIS mask so it is the same size as the NIR image. It is assumed that the pot position changes consistently between VIS and NIR image datasets. An example VIS/NIR dual pipeline to follow can be accessed online (http://plantcv.readthedocs.io/en/latest/vis_nir_tutorial/).

Object count estimation with watershed segmentation

While segmentation and analysis of whole plants in images provides useful information about plant size and growth, a more detailed understanding of plant growth and development can be obtained by measuring individual plant organs. However, fully automated segmentation of individual organs such as leaves remains a challenge, due to issues such as occlusion (Scharr et al., 2016). Multiple methods for leaf segmentation have been proposed (Scharr et al., 2016), and in PlantCV v2.0 we have implemented a watershed segmentation approach. The 'watershed_segmentation' function can be used to estimate the number of leaves for certain plant architecture types and imaging platforms (Fig. 3). The inputs required are an image, an object mask, and a minimum distance to separate object peaks. The function uses the input mask to calculate a Euclidean distance map (Liberti et al., 2014). Marker peaks calculated from the distance map that meet the minimum distance setting are used in a watershed segmentation algorithm (van der Walt et al., 2014) to segment and count the objects. Segmented objects are visualized in different colors, and the number of segmented objects is reported (Fig. 3). An example of how the watershed segmentation method was used to assess the effect of water

deficit stress on the number of leaves of Arabidopsis plants can be found in Acosta-Gamboa et al. 2017 (Acosta-Gamboa et al., 2017).

Landmarking functions for morphometrics

To extend PlantCV beyond quantification of size-based morphometric features, we developed several landmarking functions. Landmarks are generally geometric points located along the contours of a shape that correspond to homologous biological features that can be compared between subjects (Bookstein, 1991). Typical examples of landmarks include eyes between human subjects or suture joins in a skull. For a growing plant, potential landmarks include the tips of leaves and pedicel and branch angles. When specified *a priori*, landmarks should be assigned to provide adequate coverage of the shape morphology across a single dimensional plane (Bookstein, 1991). Additionally, the identification of landmark points should be repeatable and reliable across subjects while not altering their topological positions relative to other landmark positions (Bookstein, 1991). Type I landmarks provide the strongest support for homology because they are defined by underlying biological features, but it is problematic to assign Type I landmarks *a priori* when analyzing high-throughput plant imagery. To address this, PlantCV v2.0 contains functions to identify anatomical landmarks based upon the mathematical properties of object contours (Type II) and non-anatomical pseudo-landmarks/semilandmarks (Type III), as well as functions to rescale and analyze biologically relevant shape properties (Bookstein, 1991, 1997; Gunz, Mitteroecker & Bookstein, 2005; Gunz & Mitteroecker, 2013).

The 'acute' function identifies Type II landmarks by implementing a pseudo-landmark identification algorithm that operates using a modified form of chain coding (Freeman, 1961). Unlike standard chain coding methods that attempt to capture the absolute shape of a contour, the acute method operates by measuring the angle between a pixel coordinate and two neighboring pixels on opposite sides of it that fall within a set distance, or window, along the length of the contour. The two neighboring points are used to calculate an angle score for the center pixel. When the angle score is calculated for each position along the length of a contour, clusters of acute points can be identified, which can be segmented out by applying an angle threshold. The middle position within each cluster of acute points is then identified for use as a pseudo-landmark (Fig. 4A). The ability to subjectively adjust the window size used for generating angle scores also helps to tailor analyses for identifying points of interest that may differ in resolution. For example, an analysis of leaf data might utilize a larger window size to identify the tips of lobes whereas smaller window sizes would be able to capture more minute patterns such as individual leaf serrations. Further segmentation can also be done using the average pixel values output (pt_vals) for each pseudo-landmark, which estimates the mean pixel intensity within the convex hull of each acute region based on the binary mask used in the analysis. The average pixel value output allows for concave landmarks (e.g. leaf axils and grass ligules) and convex landmarks (e.g. leaf tips and apices) on a contour to be differentiated in downstream analyses. Additionally, PlantCV v2.0 includes the 'acute_vertex' function that uses the same chain code-based pseudo-landmark identification algorithm used in the 'acute' function except that it uses an adjustable local search space criteria to reduce the number of angle calculations, which speeds up landmark identification.

For Type III landmarks, the 'x_axis_pseudolandmarks' and 'y_axis_pseudolandmarks' functions identify homologous points along a single dimension of an object (x-axis or y-axis) based on equidistant point locations within an object contour. The plant object is divided up into twenty equidistant bins, and the minimum and maximum extent of the object along the axis and the centroid of the object within each bin is calculated. These sixty points located along each axis possess the properties of semi/pseudo-landmark points (an equal number of reference points that are approximately geometrically homologous between subjects to be compared) that approximate the contour and shape of the object (Fig. 4B). Such semi/pseudo-landmarking strategies have been utilized in cases where traditional homologous landmark points are difficult to assign or poorly represent the features of object shape (Bookstein, 1997; Gunz, Mitteroecker & Bookstein, 2005; Gunz & Mitteroecker, 2013).

Frequently, comparison of shape attributes requires rescaling of landmark points to eliminate the influence of size on the relative position of landmark points. The landmark functions in PlantCV output untransformed point values that can either be directly input into morphometric programs in R [shapes (Dryden & Mardia, 2016) or morpho (Schlager, Jefferis & Schlager, 2016)] or uniformly rescaled to a 0-1 coordinate system using the PlantCV 'scale_features' function. The location of landmark points can be used to examine multidimensional growth curves for a broad variety of study systems and tissue types and can be used to compare properties of plant shape throughout development or in response to differences in plant growth environment. An example of one such application is the 'landmark_reference_pt_dist' function. This function estimates the vertical, horizontal, Euclidean distance, and angle of landmark points from two landmarks (centroid of the plant object and centroid localized to the base of the plant). Preliminary evidence

from a water limitation experiment performed using a *Setaria* recombinant inbred population indicates that vertical distance from rescaled leaf tip points identified by the 'acute_vertex' function to the centroid is decreased in response to water limitation and thus may provide a proximity measurement of plant turgor pressure (Fig. 4C and 4D).

Two-class or multiclass naive Bayes classifier

Pixel-level segmentation of images into two or more classes is not always straightforward using traditional image processing techniques. For example, two classes of features in an image may be visually distinct but similar enough in color that simple thresholding is not sufficient to separate the two groups. Furthermore, even with methods that adjust for inconsistencies between images (e.g. white balancing and auto-thresholding functions), inconsistent lighting conditions in a growth chamber, greenhouse, or field can still make bulk processing of images with a single workflow difficult. Methods that utilize machine learning techniques are a promising approach to tackle these and other phenotyping challenges (Minervini, Abdelsamea & Tsaftaris, 2014; Singh et al., 2016; Ubbens & Stavness, 2017; Atkinson et al., 2017; Pound et al., 2017). With PlantCV v2.0, we have started to integrate machine learning methods to detect features of interest (e.g. the plant), starting with a naive Bayes classifier (Abbasi & Fahlgren, 2016). The naive Bayes classifier can be trained using two different approaches for two-class or multiclass (two or more) segmentation problems. During the training phase using the plantcv-train.py script, pixel RGB values for each input class are converted to the hue, saturation and value (HSV) color space. Kernel density estimation (KDE) is used to calculate a probability density function (PDF) from a vector of values for each HSV channel from each class. The output PDFs are used to parameterize the naive Bayes classifier function ('naive_bayes_classifier'), which can be used to

412 replace the thresholding steps in a PlantCV pipeline. The 'naive_bayes_classifer' function uses
413 these PDFs to calculate the probability (using Bayes' theorem) that a given pixel is in each class.
414 The output of the 'naive_bayes_classifier' is a binary image for each class where the pixels are
415 white if the probability the pixel was in the given class was highest of all classes and is black
416 otherwise. A tutorial of how to implement naive Bayes plant detection into an image processing
417 pipeline is online (http://plantcv.readthedocs.io/en/latest/machine_learning_tutorial/).
418
419 For the two-class approach, the training dataset includes color images and corresponding binary
420 masks where the background is black and the foreground (plant or other target object) is white.
421 PlantCV can be used to generate binary masks for the training set using the standard image
422 processing methods and the new 'output_mask' function. It is important for the training dataset
423 to be representative of the larger dataset. For example, if there are large fluctuations in light
424 intensity throughout the day or plant color throughout the experiment, the training dataset should
425 try to cover the range of variation. A random sample of 10% of the foreground pixels and the
426 same number background pixels are used to build the PDFs.
427
428 To assess how well the two-class naive Bayes method identifies plant material in comparison to
429 thresholding methods, we reanalyzed *Setaria* images (Fahlgren et al., 2015) using the naive
430 Bayes classifier and compared the pixel area output to pipelines that utilize thresholding steps
431 (Fig. 5). We used 99 training images (14 top view and 85 side view images) from a total of 6473
432 images. We found that the plant pixel area calculated by naive Bayes was highly correlated with
433 that calculated from pipelines that use thresholding for both side-view images (R^2=0.99; Fig. 5A)
434 and top-view images (R^2=0.96; Fig. 5B). An additional advantage to using the naive Bayes

image processing pipelines was that only five pipelines were needed to process the dataset that was originally processed with nine threshold-based pipelines.

The multiclass naive Bayes approach requires a tab-delimited table for training where each column is a class (minimum two) and each cell is a comma-separated list of RGB pixel values from the column class. We currently use the Pixel Inspection Tool in ImageJ (Schneider, Rasband & Eliceiri, 2012) to collect samples of pixel RGB values used to generate the training text file. As noted above for the two-class approach, it is important to adequately capture the variation in the image dataset for each class when generating the training text file to improve pixel classification. If images are consistent, only one image needs to be sampled for generating the training table; however, if they vary, several images may be needed. For complex backgrounds (or non-targeted objects), several classes may be required to capture all of the variation. Once the training table is generated, it is input into the plantcv-train.py script to generate PDFs for each class. As an example, we used images of wheat leaves infected with wheat rust to collect pixel samples from four classes: non-plant background, unaffected leaf tissue, rust pustule, and chlorotic leaf tissue, and then used the naive Bayes classifier to segment the images into each class simultaneously (Fig. 6). This method can likely be used for a variety of applications, such as identifying a plant under variable lighting conditions or quantifying specific areas of stress on a plant.

CONCLUSIONS

The field of digital plant phenotyping is at an exciting stage of development where it is beginning to shift from a bottleneck to one that will have a positive impact on plant research,

especially in agriculture. The Plant Image Analysis database currently lists over 150 tools that can be used for plant phenotyping [http://www.plant-image-analysis.org/; (Lobet, Draye & Périlleux, 2013)]. Despite the abundance of software packages, long-term sustainability of individual projects may become an issue due to the lack of incentives for maintaining bioinformatics software developed in academia (Lobet, 2017). In a survey of corresponding authors of plant image analysis tools by Lobet, 60% either said the tool was no longer being maintained or did not respond (Lobet, 2017). To develop PlantCV as a sustainable project we have adopted an open, community-based development framework using GitHub as a central service for the organization of developer activities and the dissemination of information to users. We encourage contribution to the project by posting bug reports and issues, developing or revising analysis methods, adding or updating unit tests, writing documentation, and posting ideas for new features. We aim to periodically publish updates, such as the work presented here, to highlight the work of contributors to the PlantCV project.

There are several areas where we envision future PlantCV development. **Standards and interoperability:** Improved interoperability of PlantCV with data providers and downstream analysis tools will require adoption of community-based standards for data and metadata [e.g. Minimum Information About a Plant Phenotyping Experiment; (Ćwiek-Kupczyńska et al., 2016)]. Improved interoperability will make it easier to develop standardized tools for statistical analysis of image processing results, both within the PlantCV project or with tools from other projects. **New data sources:** Handling and analysis of data from specialized cameras that measure three-dimensional structure or hyperspectral reflectance will require development or integration of additional methods into PlantCV. **Machine learning:** Our goal is to develop

additional tools for machine learning and collection of training data. In some cases, where these methods can be implemented in a modular and reusable framework, they can be integrated directly into PlantCV. In other cases, PlantCV can be combined with new and existing tools. A recent example of this latter approach built on PlantCV, using its image preprocessing and segmentation functions alongside a modular framework for building convolutional neural networks (Ubbens & Stavness, 2017). As noted throughout, we see great potential for modular tools such as PlantCV and we welcome community feedback.

MATERIALS & METHODS

Scripts, notebooks, and simple input data associated with the present study are available on GitHub at https://github.com/danforthcenter/plantcv-v2-paper. The image of *Arabidopsis thaliana* was captured with a Raspberry Pi computer and camera in a Conviron growth chamber. Additional details about the imaging set-up are provided in a companion paper (Tovar et al., 2017). Images of *Setaria viridis* (A10) and *Setaria italica* (B100) are from publicly available datasets that are available at http://plantcv.danforthcenter.org/pages/data.html (Fahlgren et al., 2015; Feldman et al., 2017). The image of wheat (*Triticum aestivum L.*) infected with wheat stem rust (*Puccinia graminis f. sp. tritici*) was acquired with a flatbed scanner.

Image analysis was done in PlantCV using Python v2.7.5, OpenCV v2.4.5 (Bradski, 2000), NumPy v1.12.1 (van der Walt, Colbert & Varoquaux, 2011), Matplotlib v2.0.2 (Hunter, 2007), SciPy v0.19.0 (Jones, Oliphant & Peterson), Pandas v0.20.1 (McKinney & Others, 2010), scikit-image v0.13.0 (van der Walt et al., 2014), and Jupyter Notebook v4.2.1 (Kluyver et al., 2016). Statistical analysis and data visualization was done using R v3.3 (R Core Team, 2017) and

RStudio v1.0 (RStudio Team, 2016). Graphs were produced using Matplotlib v2.0.2 (Hunter, 2007) and ggplot2 v2.2.1 (Wickham, 2009).

ACKNOWLEDGMENTS

We would like to thank Melinda Darnell, Leonardo Chavez, Kevin Reilly, and the staff of both the Danforth Center Facilities and Support Services group and the Plant Growth Facility for careful maintenance of the Danforth Center phenotyping facilities. We thank Katie Liberatore and Shahryar Kianian for images of wheat (*Triticum aestivum L.*). We would also like to thank all of the other people who have given us input on the PlantCV project in person or on GitHub.

REFERENCES

Abbasi A., Fahlgren N. 2016. Naive Bayes pixel-level plant segmentation. In: *2016 IEEE Western New York Image and Signal Processing Workshop (WNYISPW)*. 1–4. DOI: 10.1109/WNYIPW.2016.7904790.

Acosta-Gamboa LM., Liu S., Langley E., Campbell Z., Castro-Guerrero N., Mendoza-Cozatl D., Lorence A. 2017. Moderate to severe water limitation differentially affects the phenome and ionome of Arabidopsis. *Functional plant biology: FPB* 44:94–106. DOI: 10.1071/FP16172.

Atkinson JA., Lobet G., Noll M., Meyer PE., Griffiths M., Wells DM. 2017. Combining semi-automated image analysis techniques with machine learning algorithms to accelerate large scale genetic studies. *GigaScience*. DOI: 10.1093/gigascience/gix084.

Bookstein FL. 1991. Morphometric tools for landmark data Cambridge University Press. *New York*.

Bookstein FL. 1997. *Morphometric Tools for Landmark Data: Geometry and Biology*.

Cambridge University Press.

Bradski G. 2000. The opencv library. *Doctor Dobbs Journal* 25:120–126.

Ćwiek-Kupczyńska H., Altmann T., Arend D., Arnaud E., Chen D., Cornut G., Fiorani F., Frohmberg W., Junker A., Klukas C., Lange M., Mazurek C., Nafissi A., Neveu P., van Oeveren J., Pommier C., Poorter H., Rocca-Serra P., Sansone S-A., Scholz U., van Schriek M., Seren Ü., Usadel B., Weise S., Kersey P., Krajewski P. 2016. Measures for interoperability of phenotypic data: minimum information requirements and formatting. *Plant methods* 12:44. DOI: 10.1186/s13007-016-0144-4.

Dryden IL., Mardia KV. 2016. *Statistical Shape Analysis: With Applications in R*. John Wiley & Sons.

Duarte M. 2015. Notes on scientific computing for biomechanics and motor control. *GitHub repository*.

Dudley JT., Butte AJ. 2009. A quick guide for developing effective bioinformatics programming skills. *PLoS Computational Biology* 5:e1000589. DOI: 10.1371/journal.pcbi.1000589.

Fahlgren N., Feldman M., Gehan MA., Wilson MS., Shyu C., Bryant DW., Hill ST., McEntee CJ., Warnasooriya SN., Kumar I., Ficor T., Turnipseed S., Gilbert KB., Brutnell TP., Carrington JC., Mockler TC., Baxter I. 2015. A versatile phenotyping system and analytics platform reveals diverse temporal responses to water availability in Setaria. *Molecular Plant* 8:1520–1535. DOI: 10.1016/j.molp.2015.06.005.

Fahlgren N., Gehan MA., Baxter I. 2015. Lights, camera, action: high-throughput plant phenotyping is ready for a close-up. *Current Opinion in Plant Biology* 24:93–99. DOI: 10.1016/j.pbi.2015.02.006.

Feldman MJ., Paul RE., Banan D., Barrett JF., Sebastian J., Yee M-C., Jiang H., Lipka AE.,

Brutnell TP., Dinneny JR., Leakey ADB., Baxter I. 2017. Time dependent genetic analysis links field and controlled environment phenotypes in the model C4 grass Setaria. *PLoS Genetics* 13:e1006841. DOI: 10.1371/journal.pgen.1006841.

Freeman H. 1961. On the encoding of arbitrary geometric configurations. *IRE Transactions on Electronic Computers* EC-10:260–268. DOI: 10.1109/TEC.1961.5219197.

Furbank RT., Tester M. 2011. Phenomics--technologies to relieve the phenotyping bottleneck. *Trends in Plant Science* 16:635–644. DOI: 10.1016/j.tplants.2011.09.005.

Gonzalez RC., Woods RE. 2002. *Digital Image Processing*. Prentice Hall.

Gunz P., Mitteroecker P. 2013. Semilandmarks: a method for quantifying curves and surfaces. *Hystrix, the Italian Journal of Mammalogy* 24:103–109.

Gunz P., Mitteroecker P., Bookstein FL. 2005. Semilandmarks in Three Dimensions. In: Slice DE ed. *Modern Morphometrics in Physical Anthropology*. Developments in Primatology: Progress and Prospects. Springer US, 73–98. DOI: 10.1007/0-387-27614-9_3.

Hunter JD. 2007. Matplotlib: A 2D graphics environment. *Computing in Science & Engineering* 9:90–95. DOI: 10.1109/MCSE.2007.55.

Jones E., Oliphant T., Peterson P. *SciPy: Open source scientific tools for Python*.

Kaehler A., Bradski G. 2016. *Learning OpenCV 3: Computer Vision in C++ with the OpenCV Library*. O'Reilly Media, Inc.

Kluyver T., Ragan-Kelley B., Pérez F., Granger B., Bussonnier M., Frederic J., Kelley K., Hamrick J., Grout J., Corlay S., Ivanov P., Avila D., Abdalla S., Willing C., Jupyter Development Team. 2016. Jupyter Notebooks – a publishing format for reproducible computational workflows. In: Loizides F, Schmidt B eds. *Positioning and Power in Academic Publishing: Players, Agents and Agendas: Proceedings of the 20th International*

Conference on Electronic Publishing. Amsterdam: IOS Press, 87–90. DOI: 10.3233/978-1-61499-649-1-87.

Liberti L., Lavor C., Maculan N., Mucherino A. 2014. Euclidean Distance Geometry and Applications. *SIAM Review* 56:3–69. DOI: 10.1137/120875909.

Lobet G. 2017. Image analysis in plant sciences: Publish then perish. *Trends in Plant Science*. DOI: 10.1016/j.tplants.2017.05.002.

Lobet G., Draye X., Périlleux C. 2013. An online database for plant image analysis software tools. *Plant Methods* 9:38. DOI: 10.1186/1746-4811-9-38.

Mangalam H. 2002. The Bio* toolkits--a brief overview. *Briefings in Bioinformatics* 3:296–302. DOI: 10.1093/bib/3.3.296.

McKinney W., Others. 2010. Data structures for statistical computing in python. In: *Proceedings of the 9th Python in Science Conference*. SciPy Austin, TX, 51–56.

Millman KJ., Aivazis M. 2011. Python for Scientists and Engineers. *Computing in Science & Engineering* 13:9–12. DOI: 10.1109/MCSE.2011.36.

Minervini M., Abdelsamea MM., Tsaftaris SA. 2014. Image-based plant phenotyping with incremental learning and active contours. *Ecological Informatics* 23:35–48. DOI: 10.1016/j.ecoinf.2013.07.004.

Oliphant TE. 2007. Python for scientific computing. *Computing in Science & Engineering* 9:10–20. DOI: 10.1109/MCSE.2007.58.

Otsu N. 1979. A threshold selection method from gray-level histograms. *IEEE Transactions on Systems, Man, and Cybernetics* 9:62–66.

Pauli D., Chapman SC., Bart R., Topp CN., Lawrence-Dill CJ., Poland J., Gore MA. 2016. The quest for understanding phenotypic variation via integrated approaches in the field

environment. *Plant Physiology* 172:622–634. DOI: 10.1104/pp.16.00592.

Perez-Riverol Y., Gatto L., Wang R., Sachsenberg T., Uszkoreit J., Leprevost F da V., Fufezan C., Ternent T., Eglen SJ., Katz DS., Pollard TJ., Konovalov A., Flight RM., Blin K., Vizcaíno JA. 2016. Ten simple rules for taking advantage of Git and GitHub. *PLoS Computational Biology* 12:e1004947. DOI: 10.1371/journal.pcbi.1004947.

Pound MP., Atkinson JA., Townsend AJ., Wilson MH., Griffiths M., Jackson AS., Bulat A., Tzimiropoulos G., Wells DM., Murchie EH., Pridmore TP., French AP. 2017. Deep Machine Learning provides state-of-the-art performance in image-based plant phenotyping. *GigaScience*. DOI: 10.1093/gigascience/gix083.

R Core Team. 2017. R: A Language and Environment for Statistical Computing.

RStudio Team. 2016. *RStudio: Integrated Development Environment for R*. Boston, MA: RStudio, Inc.

Scharr H., Minervini M., French AP., Klukas C., Kramer DM., Liu X., Luengo I., Pape J-M., Polder G., Vukadinovic D., Yin X., Tsaftaris SA. 2016. Leaf segmentation in plant phenotyping: a collation study. *Machine Vision and Applications* 27:585–606. DOI: 10.1007/s00138-015-0737-3.

Schlager S., Jefferis G., Schlager MS. 2016. Package "Morpho."

Schneider CA., Rasband WS., Eliceiri KW. 2012. NIH Image to ImageJ: 25 years of image analysis. *Nature Methods* 9:671–675.

Singh A., Ganapathysubramanian B., Singh AK., Sarkar S. 2016. Machine learning for high-throughput stress phenotyping in plants. *Trends in Plant Science* 21:110–124. DOI: 10.1016/j.tplants.2015.10.015.

Tovar JC., Hoyer JS., Lin A., Tielking A., Tessman M., Miller M., Callen ST., Castillo SE.,

Fahlgren N., Carrington JC., Nusinow DA., Gehan MA. 2017. Raspberry Pi powered imaging for plant phenotyping. *Applications in Plant Sciences* submitted.

Ubbens JR., Stavness I. 2017. Deep Plant Phenomics: A deep learning platform for complex plant phenotyping tasks. *Frontiers in Plant Science* 8:1190. DOI: 10.3389/fpls.2017.01190.

van der Walt S., Colbert SC., Varoquaux G. 2011. The NumPy array: A structure for efficient numerical computation. *Computing in Science & Engineering* 13:22–30. DOI: 10.1109/MCSE.2011.37.

van der Walt S., Schönberger JL., Nunez-Iglesias J., Boulogne F., Warner JD., Yager N., Gouillart E., Yu T., scikit-image contributors. 2014. scikit-image: image processing in Python. *PeerJ* 2:e453. DOI: 10.7717/peerj.453.

Wickham H. 2009. *ggplot2: Elegant Graphics for Data Analysis*. Springer New York.

Wilson G., Aruliah DA., Brown CT., Chue Hong NP., Davis M., Guy RT., Haddock SHD., Huff KD., Mitchell IM., Plumbley MD., Waugh B., White EP., Wilson P. 2014. Best practices for scientific computing. *PLoS Biology* 12:e1001745. DOI: 10.1371/journal.pbio.1001745.

Zack GW., Rogers WE., Latp SA. 1977. Automatic measurement of sister chromatid exchange frequency. *Journal of Histochemistry and Cytochemistry* 25:741–753.

FIGURE 1

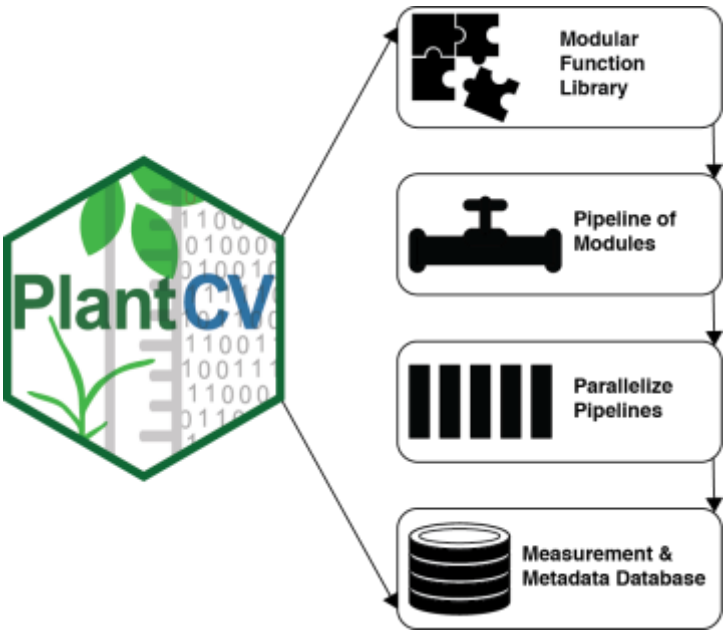

Figure 1: Diagram of the components of PlantCV.

PlantCV is an open-source, open-development suite of image analysis tools. PlantCV contains a library of modular Python functions that can be assembled into simple sequential or branching/merging processing pipelines. Image processing pipelines, which process single images (possibly containing multiple plants), can be deployed over large image sets using PlantCV parallelization, which outputs an SQLite database of both measurements and image/experimental metadata.

651 **FIGURE 2**

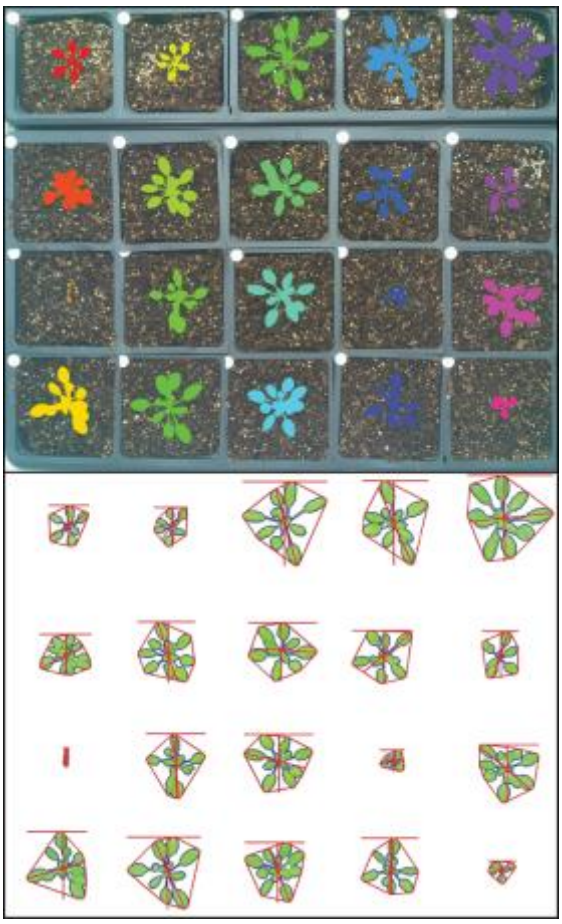

652

653 **Figure 2: Analysis of images containing multiple plants.**

654 New functions have been added to PlantCV v2.0 that enable individual plants from images
655 containing multiple plants to be analyzed. The ‘cluster_contours’ function clusters contour
656 objects using a flexible grid arrangement (approximate rows and columns defined by a user). The
657 top image, produced by ‘cluster_contours’ in debug mode, highlights plants by their cluster
658 group with unique colors on a sequential scale. The ‘cluster_contours_split_img’ function creates
659 a new image for each cluster group. The resulting images of individual plants can be processed
660 by standard PlantCV methods. In the bottom image, the ‘cluster_contours_split_img’ function
661 was used to split the full image into individual plants. The shape of each plant was then analyzed
662 with ‘analyze_objects’ and printed on a common image background.

663 **FIGURE 3**

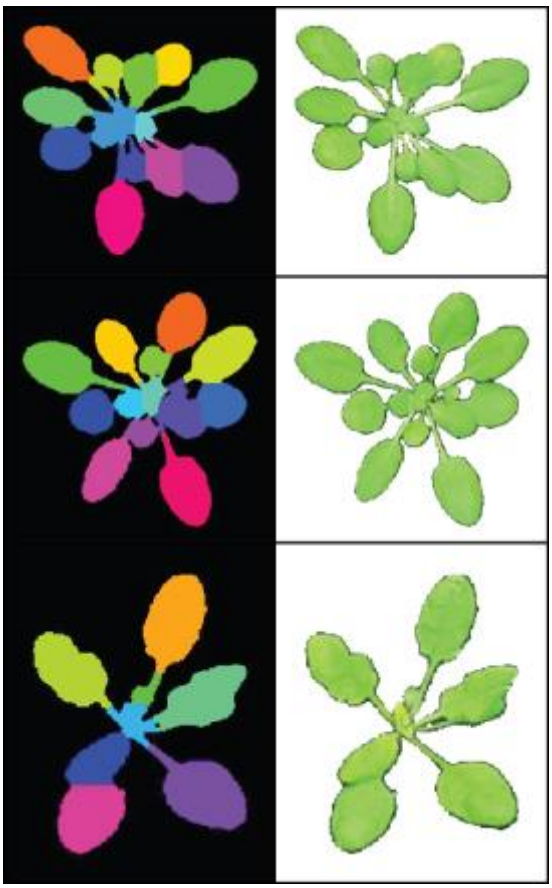

664

665 **Figure 3: Leaf segmentation by a distance-based watershed transformation.**

666 The watershed segmentation function can be used to segment and estimate the number of objects
667 in an image. For the three example images, the watershed segmentation function was used to
668 estimate the number of leaves for *Arabidopsis thaliana* (estimated leaf count for top: 13, middle:
669 14, and bottom: 8). Images shown are the output from the 'watershed_segmentation' function
670 (left) and the segmented plants (right).

671

672

673

674

675 **FIGURE 4**

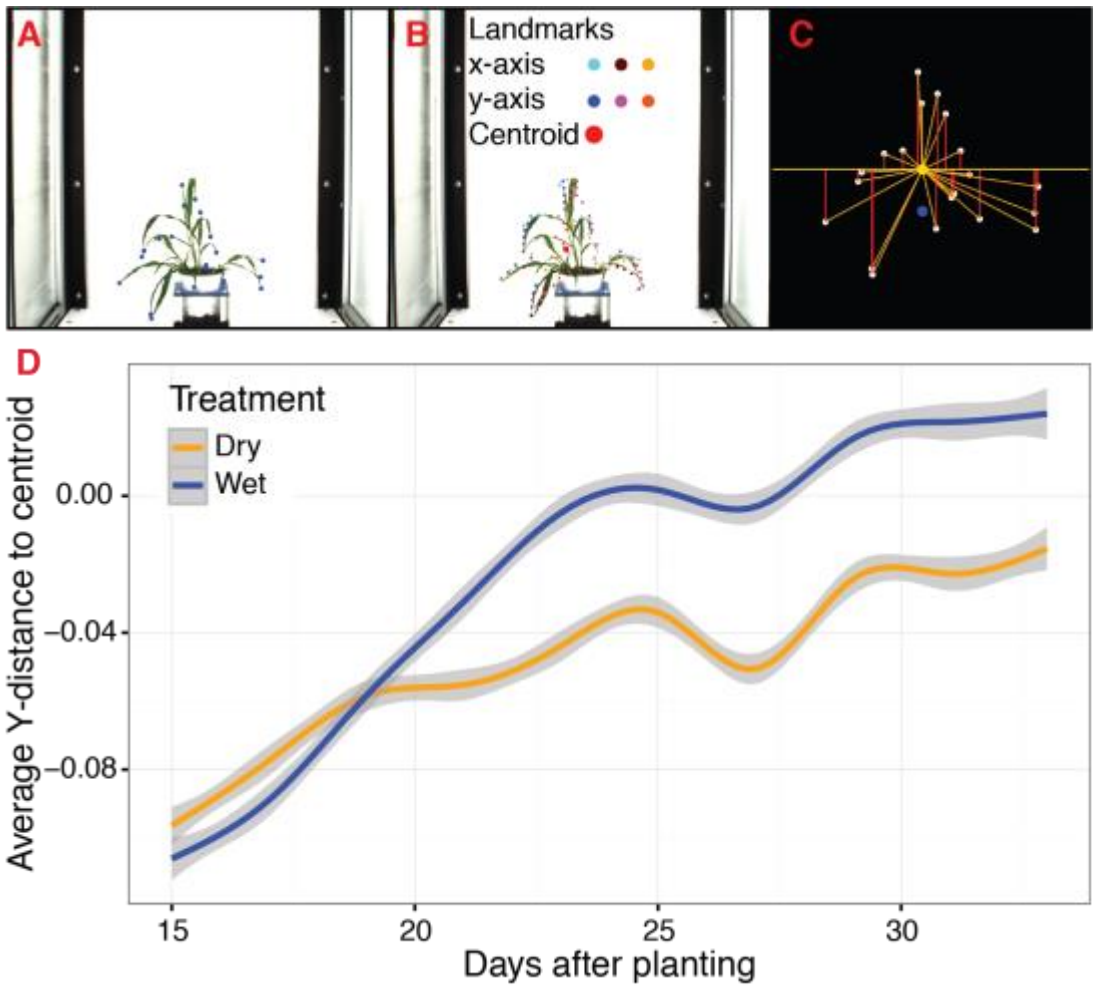

676

677 **Figure 4: Landmark-based analysis of plant shape in PlantCV.**

678 A) Automatic identification of leaf tip landmarks using the 'acute' and 'acute_vertex' functions
679 (blue dots). B) Geometrically homologous semi/pseudo-landmarks across both the x- and y-axes.
680 Semi/pseudo-landmarks identified by scanning the x-axis are denoted by light blue (top side of
681 the contour), brown (bottom side of the contour), and light orange (centroid location of
682 horizontal bins) dots. Semi/pseudo-landmarks identified by scanning the y-axis are denoted by
683 dark blue (left side of the contour), pink (right side of the contour), and dark orange (centroid
684 location of vertical bins) dots. The plant centroid is plotted larger in red. C) A representation of
685 the rescaled plant landmarks identified in panel (A). White points correspond to the leaf tips. The

686 orange point is the location of the plant centroid. The blue point is the location of the plant
687 centroid where the plant emerges from the soil. Red lines are the vertical distance from leaf tip
688 points relative to the plant centroid. D) Analysis of the average scaled vertical distance from each
689 leaf tip to the centroid diverges in response to water limitation.

690 **FIGURE 5**

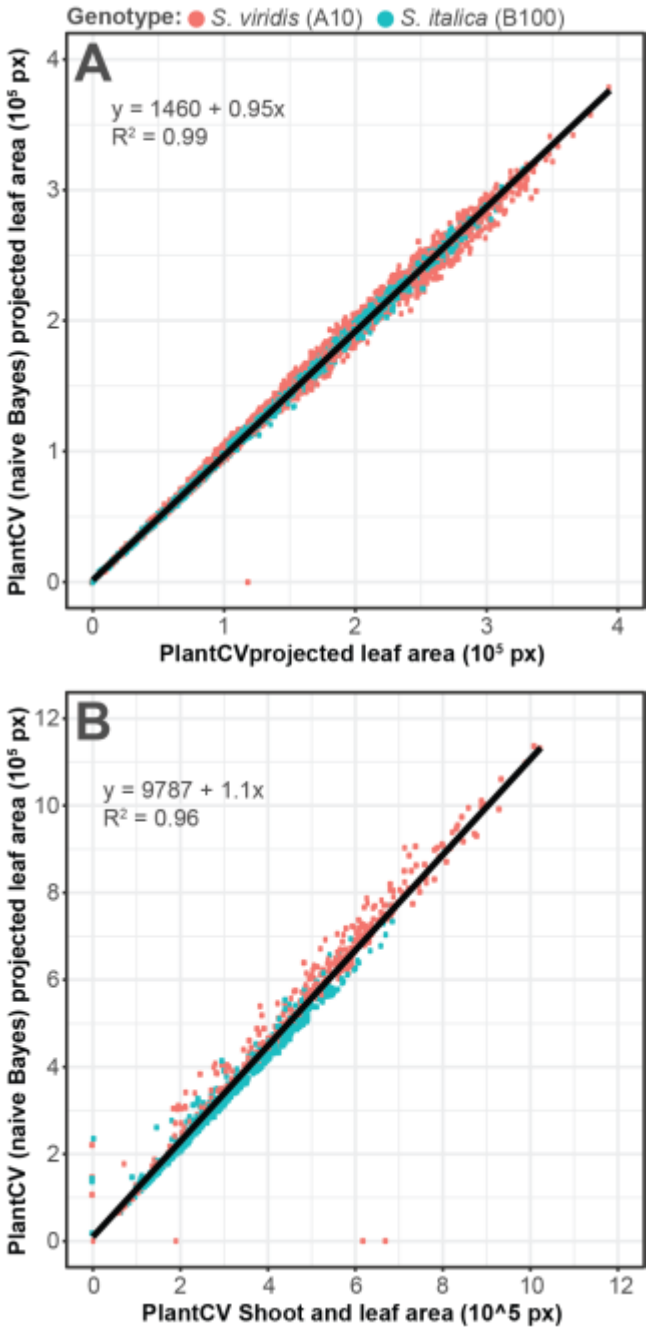

691

692 **Figure 5: Plant segmentation using a naive Bayes classifier.**

693 Correlation between plant area (pixels) detected using thresholding pipelines (Fahlgren et al.,

694 2015) on the x-axis compared to plant area detected using a trained naive Bayes classifier on the

695 y-axis. A) Side-view images. B) Top-view images.

FIGURE 6

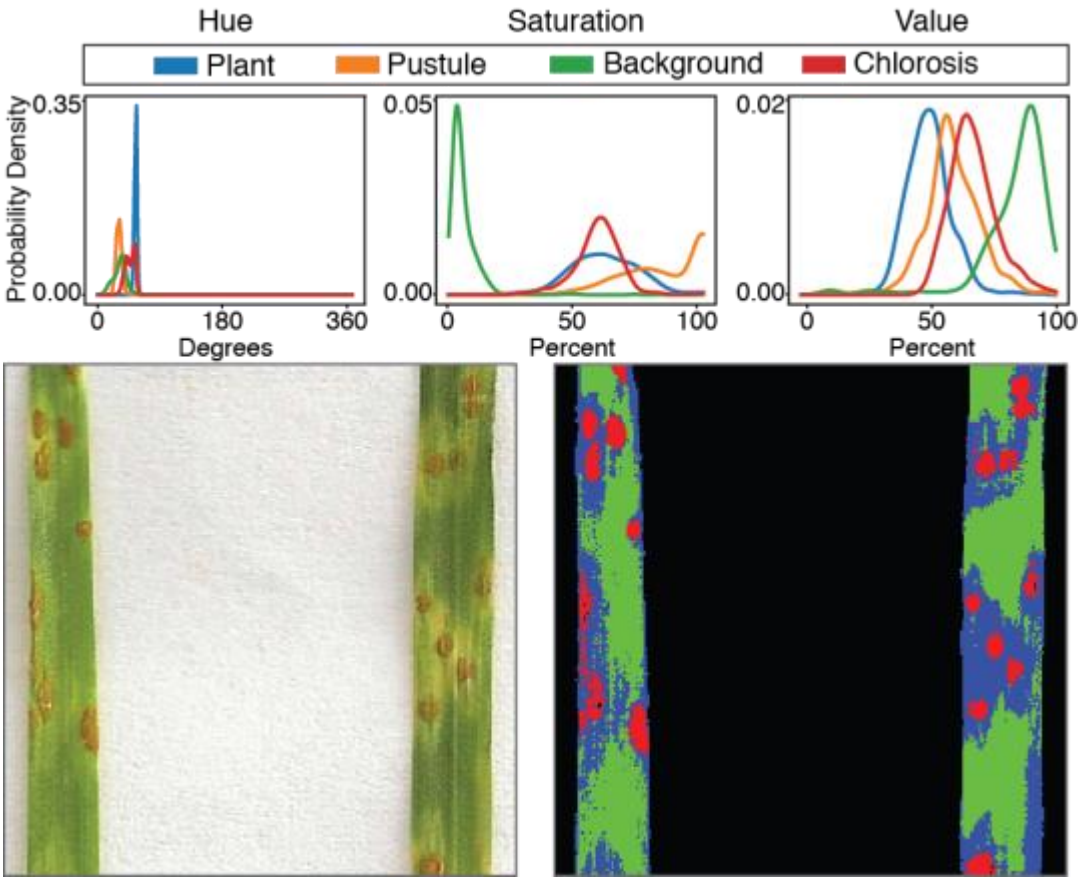

Figure 6: Simultaneous segmentation of four feature groups using the naive Bayes classifier.

An example of the naive Bayes classifier used to assign pixels into 4 classes: background, unaffected plant tissue, chlorotic tissue, and wheat stem rust pustules. (Top) Probability density functions (PDFs) from the 'plantcv-train.py' script that show hue, saturation, and value color channel distributions of four classes estimated from training data. (Bottom) Example of a classified image with the original image (left) and merged pseudocolored image (right) with pixels classified by the 'naive_bayes_classifier' as background (black), unaffected leaf tissue (green), chlorotic leaf tissue (blue), and pustules (red).